Novel Control Strategy for Standalone Wind Energy Conversion System Supplying Power to Isolated DC Load

Devashish Jha[1*], Amarnath Thakur[2]
1- Department of EEE, National Institute of Technology Jamshedpur, India.
Email: devashish.sit@gmail.com (Corresponding author)
2- Department of EEE, National Institute of Technology Jamshedpur, India.
Email:anthakur@gmail.com

Received: February 2018 Revised: April 2018 Accepted: June 2018

ABSTRACT:
This research paper has aimed to provide an insight into developing a control strategy for a standalone wind energy conversion system (SWECS) intended to power a DC load. The system mainly consists of the wind turbine (WT), generator, power electronics devices, battery bank, and its charging control circuit along with pitch angle control of wind turbine. Charging of battery is attained through tip-speed ratio (TSR) MPPT logic. DC-DC converter acts as a charge controller which charges the battery in a controlled way. Pitch angle control mechanism generates appropriate pitch angle command to dampen the rotational speed of the wind turbine. It limits the turbine output power, generator speed and rectifier output voltage during high wind speed ensuring electrical and mechanical safety of the wind turbine. The three-phase self- excited induction generator (SEIG) coupled with a wind turbine is used to produce electrical power. It is connected to load via the AC-DC-DC converter to obtain regulated voltage at the load side. The efficacy of control logic developed for proposed wind energy conversion system is tested in MATLAB/Simulink platform varying wind and load profile.

KEYWORDS: Wind Energy Conversion System (WECS), Pitch Control, Maximum Power Point Tracking (MPPT), Wind Turbine (WT), Charge Controller.

1. INTRODUCTION

Wind has been used for ages as an alternative source of energy. It has become more popular in recent years, because of technological innovations and the rise of interest in clean energy sources [1-3]. Wind energy conversion system (WECS) transforms wind energy into electrical energy using a WT coupled with generator by running it above synchronous speed. Despite remarkable growth, there are still many challenges before the researcher mainly caused by unpredictable nature of wind. Small-scale standalone wind turbines (WTs) ranging in power rating from a few hundred watts to a hundred kilowatts, mainly engaged for off-grid applications are getting ample consideration for the location where access of grid is not possible. It provides a very attractive solution in the form of electrical energy for remote communities where abundance of wind energy is available. Although the main principles of operation are the same in on-grid and off-grid, connection of WECS to the grid allows for extracting the maximum available power from wind resources at any moment of time. In contrast, for an off-grid Wind WECS, one of the major challenges is to meet the demand of the load that varies with time and maintains the power balance. Therefore, appropriate selection of associated controller is a very important aspect for successful operation of WECS. Both synchronous and asynchronous machine are used as wind turbine generator in WECS. However, before selecting the generators, it is very much essential to study the operation of the generator and the status of the system of which the generator will be a part. A detailed comparison on selection of WT generator is made in [4]. The synchronous machine is particularly suitable for high capacities, whereas asynchronous one is more suitable for low capacity wind power generation. Asynchronous machine (induction generator) is a viable choice as the WT generator since it is low-priced with having robust construction compared to permanent magnet synchronous generator (PMSG), needs little maintenance compared to wound rotor synchronous generator and double fed induction generator [5, 6]. Ability of induction generator to produce power at varying speed makes it preferred choice for standalone application where connection to the grid is not possible. In standalone application, there is requirement of suitably valued capacitor bank connected across the stator terminals of the generator. Such an arrangement is

called self-excited induction generator (SEIG). The prime advantage of using SEIG is its capability to generate electric power over a wide range of speeds. This enables the wind turbine to run at its peak efficiency for a wide range of wind speeds and extract maximum wind power available. Although SEIG has numerous benefits, it is subjected to poor voltage regulation owing to the inequality between the reactive power supplied by the capacitor bank and that required by the load and machine [7]. Therefore, the accurate choice of the capacitance is crucial in fixing both the stator voltage and frequency at the required value. The time-varying generated ac power output of SEIG is difficult to control as it is dependent upon highly intermittent wind profile. Therefore, in order to get regulated supply WECS is interfaced with suitable power electronics converter [8, 24]. The generated ac power is rectified to dc via three-phase diode bridge rectifier. Intermittency in the wind flow has caused the requirement for an efficient energy backup to counter any power imbalance between load and generation unit. Battery is one of the reliable energy backup that may be useful in supplying power in the case of unavailability of sufficient wind power [9].

In the pursuit of capturing the maximal available power from wind, the maximum power point tracking (MPPT) algorithm/technique is applied. MPPT enhances the efficiency for conversion of power by varying the turbine rotor speed as per the real wind speeds. Therefore, a wakeful selection and effective application of the MPPT technique are essential to improve the efficiency of a particular WECS. Several maximum power point algorithms/techniques (MPPT) are available in literature with their own merits and demerits [10, 11]. Some of the popular are: perturb and observe (P&O) control, optimum relation based (ORB) and tip speed ratio (TSR) control.

P&O control compares the difference between two successive turbine output powers on perturbation and regulates the turbine angular speed [12]. This algorithm does not demand information of the system and is completely independent of the WT, generator, and wind features. Therefore, it works without device (anemometer) for wind speed measurement making the system simple. The main drawback of P&O control algorithm is its slow response, especially for a high inertial wind turbine system. Rapidly changing nature of wind flow makes the situation even worse [13]. In the normal P&O control method, the direction of the subsequent perturbation, is determined by the change in power due to the prior perturbation. As the P&O control is ignorant to the sudden change in environmental condition, this rule can be ambiguous, since the direction of perturbation might be governed by the variation in wind velocity instead of the perturbation applied. In ORB control method, the peak power point is traced with the help of optimum established relationship between system parameters such as shaft speed or torque versus power [14, 15]. In [16], a fresh intermediate variable β is presented, whose value at peak power point can be expressed in terms of known parameters of the wind turbine system. It can be noted that peak power increases with an increase in wind speed, however value of β at peak power point remains unchanged with a change in wind velocity as it is based on WT system parameter. This observation is taken into account for forming MPPT algorithm. The prime weakness of ORB control is the requirement for past information of the exact system parameters that differ from system to system.

In tip-speed ratio (TSR) control algorithm, there is a need to keep TSR of the wind turbine at its optimum value so that extracted power from wind could be maximized. TSR is the ratio between tangential speed of the tip of the WT blade V_{tip} and wind speed. this algorithm needs wind speed to be measured to catch the optimum TSR of the turbines. It has a straightforward approach with high efficiency and fast response to the wind speed variations [17]. Standalone WECS in general, needs two separate power converter circuitry to achieve the MPPT function for supplying maximum possible power to load and to control the charging rate of the battery bank. In [18], buck type MPPT charger is proposed that operates in two battery charging operating mode, constant voltage mode (CVM) and pulsating current mode (PCM). Charging is done in discontinuous mode (DCM), causing discontinuous charging of the battery. It is shown that there is protection for overpower and turbine over speed. However, overcharging protection for the battery seems somewhat difficult to achieve accurately, as charging of battery in DCM mode is realized through MPPT that is highly parameter independent. In addition, paper does not incorporate discussion on pitch angle control to provide mechanical and electrical safety to the WT. When the speed of wind goes beyond the rated value, output power must be confined by changing the pitch angle of WT in order to reduce aerodynamic efficiency. Many techniques are found in various literature explaining about different pitch control techniques [19-22]. In paper [19-21] control strategy is developed for pitch angle control of an SCIG coupled wind turbine so as to achieve required output power and improve performance by exploiting the ability of fuzzy and PI/PID control techniques. In [21], the author has proposed the pitch controller that ensures WT parameters (power, speed) and the rectifier output dc voltage are maintained between their maximum permissible bounds to guarantee operation of the WECS lie within their safe limit. However, there lack a discussion on tuning method for proper selection of parameter for controller. In the paper [22], a Fuzzy logic based pitch angle control approach based is suggested for the variable-speed WECS. However, it has

considered PMSG as WT generator (WTG) for the grid connected system.

After going through aforesaid literature it can be observed that standalone application of WT is getting wide attention these days for supplying power to isolated load. To track maximum power from varying wind profile, the MPPT technique is used with [18] and without taking consideration of battery/energy storage into the system. However [18], does not incorporate pitch control, a technique essential for ensuring electrical and mechanical safety of WT. In [21], integrated action of MPPT scheme with battery charging control and pitch angle control is implemented to meet the requirement of dc load under varying wind and load profile. Though, in this paper, method for selection of various parameter of controller and compensator is not discussed. Moreover, while implementing MPPT through Tip speed ratio (TSR) control, method to find value of optimal TSR is completely ignored.

The paper is structured as follows, a detailed explanation of the proposed standalone wind energy conversion system (SWECS) supplying power to a dc load is presented section 2. Modelling of SEIG, aerodynamics of WT and method to find optimal TSR have found space in section 2. The combined action of control consisting of the charge controller of battery through TSR tracking and pitch angle controller for the WT blade is deliberated in Section 3. It is shown that charging control is achieved through tip-speed ratio MPPT control. Section 4 describes proposed pitch control strategy for the wind turbine. Section 5 is devoted to result and discussion. The Effectiveness of the control schemes of the system supplying power to dc load is shown by varying wind speed and load profile. At last, Section 6 concludes the paper.

2. SYSTEM DESCRIPTION

The proposed WECS consist of a horizontal axis wind turbine (WT), and battery bank of 500 Ah. The WECS is intended to power varying (0-4 kW) isolated dc load. The load is modelled such that it requires regulated voltage of 50 volts. The WT is coupled with 5.4 hp (≃ 4kW) SEIG. Since the system is isolated, capacitors bank is connected across stator terminal of SEIG to fulfil reactive ac excitation current demand for its operation. Generated ac power is sent to load via ac-dc-dc converter to ensure regulated power supply at load side. Three phase diode bridge rectifier (DBR) convert variable magnitude, variable frequency voltage at the stator terminal into varying dc output voltage. Because of having high reliability, low cost and simple circuit, DBR is used in place of a controlled rectifier. Battery is introduced into the system to meet the power requirement of dc load in the event of insufficient flow of the wind. The composite system (WECS including battery) needs to be interfaced with load through appropriate control logic. Charging and discharging of battery is controlled by dc –dc converter. Control strategy takes the help of TSR- MPPT technique and tries to charge the battery at the earliest while taking the cognisance of battery state of charge (SoC).

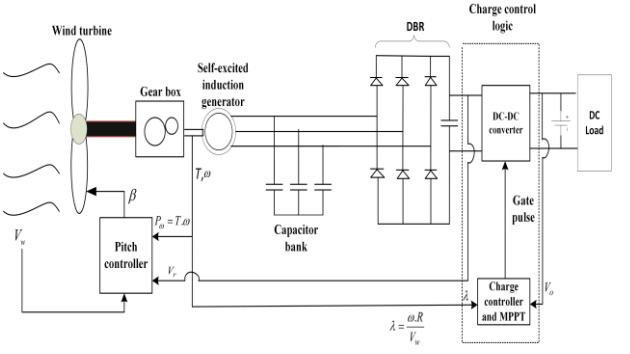

Fig. 1. Layout of the proposed standalone wind energy conversion system along with the control logic circuit.

An important role of the battery is to maintain the load terminal voltage at fixed level irrespective of the fact whether it is charging or discharging. To keep the turbine operation within permissible limit and ensuring the turbine electrical and mechanical safety, pitch control logic is incorporated. The combined action of battery charging and pitch control confirm satisfactory performance of the entire standalone WECS. The plan for the whole system is depicted in Fig. 1.

2.1. Wind/ Wind Turbine Aerodynamic Characteristics

Wind flowing with speed $\boldsymbol{V_w}$ falling at swept area of WT blade contains the mechanical powers [16],

$$P_w = 0.5\,\rho.\pi.R^2.V_w^3 \tag{1}$$

Where ρ the density of wind and R is the radius of the circular path in which tip of blade rotate. The power seized by the blades of the WT, P_{blade} is:

$$P_{blade} = 0.5\,\rho.\pi.R^2.V_w^3 C_p(\lambda,\beta) \tag{2}$$

C_p Being the function of tip-speed ratio, λ and pitch angle, β, is temed as power coefficient or efficiency of the WT and expressed as,

$$C_p(\lambda,\beta) = 0.73\left[\frac{151}{\lambda_i} - 0.58\beta - 0.002\beta^{2.14} - 13.20\right] e^{-18.40/\lambda_i} \tag{3}$$

λ_i is defined by the following equation,

$$\lambda_i = \left(\frac{1}{\lambda - 0.02\beta} - \frac{0.003}{\beta^3 + 1} \right)^{-1} \quad (4)$$

Tip-speed ratio (TSR) may be expressed as ratio between tangential speed of the tip of the WT blade V_{tip} and wind speed.

$$\lambda = \frac{R.\omega_r}{V_w} \quad (5)$$

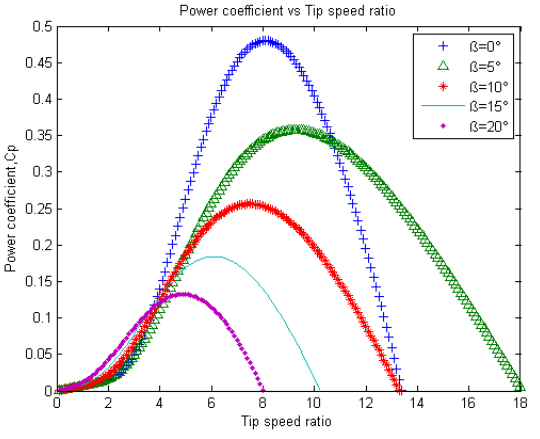

Fig. 2. Typical power coefficient vs Tip speed ratio (λ)curve.

Turbine mechanical torque is given by,

$$T_m = 0.5\rho.\pi.R^2.V_w{}^3.C_p(\lambda,\beta).(1/\omega_r) \quad (6)$$

For a given wind speed, the power extracted from the wind is maximized at the peak value of C_p. The optimum value of C_p always occurs at particular value of TSR (λ). This implies that under varying wind speed condition, rotor speed should be adjusted accordingly such that value of λ is maintained at some particular value. On the basis of the above aforementioned equation, characteristic curve showing relation with power coefficient versus TSR curve is presented in Fig. 2. It can easily be observed that with increase in pitch angle of turbine blade, power coefficient decreases as the angular velocity of turbine blade. This feature is useful in designing the pitch control technique for reducing the output power by changing the pitch angle at varying wind speeds.

2.2. Determination of Optimal TSR (λ_{opt})

Fig. 2 displays the power coefficient *versus* tip speed ratio curve. To capture the maximum power, the wind system need to be operated at the top point of the curve regardless of the wind speed. To achieve this aim, speed of WT blade ought to be adjusted in a manner such that the TSR corresponds to maximum power point (MPP). Therefore, for employing MPPT using TSR of the turbine, it is cumbersome to find the value of optimum TSR corresponding to maximum power point.

Differentiating (2) with respect to turbine speed,

$$\frac{dP_{blade}}{d\omega_r} = 0.5\rho.\pi R^2.v_\omega{}^3 \frac{dc_p}{d\omega_r} \quad (7)$$

As, $\frac{dC_p}{d\omega} = (dc_p / d\lambda_i)(d\lambda_i / d\omega_r)$

Thus (7) can be written as,

$$\frac{dP_{blade}}{d\omega_r} = 0.5\rho.A.v_\omega{}^3.(dc_p / d\lambda_i)(d\lambda_i / d\omega_r) \quad (8)$$

Differentiating (3) with respect to λ_i produces,

$$\frac{dC_p(\lambda,\beta)}{d\lambda_i} = \left[\frac{-110.20}{\lambda_i^2} + \frac{2028.20}{\lambda_i^3} - \frac{18.40\mu}{\lambda_i^2} \right].e^{-18.4/\lambda_i} \quad (9)$$

Where, $\mu = 0.4234\beta + 0.002\beta^{2.14} + 9.63$,

Differentiating (4) with respect to ω_r produces.

$$\frac{d\lambda_i}{d\omega_r} = \frac{V_w.R[\eta(\beta^3+1) - 0.003\sigma}{(V_w.\eta - 0.003R.\omega_r)^2} \quad (10)$$

Where, $\eta = 1 + 0.00006\beta + \beta^3$ and

$\sigma = 0.02(1+\beta^3)\beta$

From (7)-(10), we have,

$$\frac{dP_{blade}}{d\omega_r} = 0.5\rho AV_\omega{}^3.\left[\frac{-110.20}{\lambda_i^2} + \frac{2028.20}{\lambda_i^3} - \frac{18.40\mu}{\lambda_i^2} \right].$$
$$\left[e^{-18.4/\lambda_i}.\frac{V_w.R[\eta(\beta^3+1) - 0.003\sigma}{(V_w.\eta - 0.003R.\omega_r)^2} \right] \quad (11)$$

To locate the maximum power point for finding corresponding angular velocity of the WT, equation (11) is equated to zero, gives value of turbine angular speed at the MPP.

$$\omega_r(peak) = \frac{V_w}{R}.\left[\frac{2028.20\eta + \sigma(110.20 + 18.40\mu)}{(\beta^3+1).(110.20 + 18.40\mu) + 6.07} \right] \quad (12)$$

Taking, $\beta = 0$, $\eta = 1, \sigma = 0$ and $\mu = 9.63$.
From (12),

$$\omega_r = \frac{V_w}{R}.[6.911] \quad (13)$$

Therefore,
Optimal TSR

$$(\lambda_{opt}) = \frac{R.\omega_r}{V_w} = 6.911 \simeq 7 \quad (14)$$

2.3. Modelling of Self –excited Induction Generator

Selection of the frame of reference for modelling of the SEIG is basically decided on the basis of its operation. Generally, for the case of unbalanced or discontinuous stator voltage, stationary frame of reference is chosen to model SEIG [23].

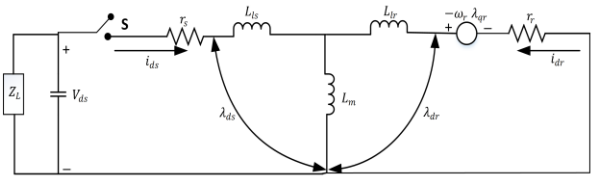

(a)

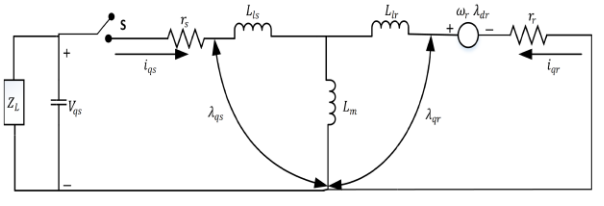

(b)

Fig. 3. d-q model of SEIG (a) d-axis (b) q axis

For the representation of an induction machine (IM) model in stationary frame, the d-q arbitrary reference frame model of machine is transformed into stationary reference frame. The d-q model of the SEIG in the stationary reference frame is found by substituting $\omega = 0$ in the arbitrary reference frame equivalent of the IM shown in Fig. 3. For the excitation purpose, capacitors of appropriate values are connected across the stator terminals of an IM. The voltage will be induced and slowly starts building up to reach a steady-state value. Rearranging the terms after writing loop equations for Fig. 3, the mathematical equations describing SEIG model can be expressed in stationary frame of reference as follows:

$$V_{ds} = r_s.i_{ds} + p\lambda_{ds} \quad (15)$$
$$V_{qs} = r_s.i_{qs} + p\lambda_{qs} \quad (16)$$
$$V_{dr} = r_r.i_{dr} + p\lambda_{dr} + \omega_r \lambda_{qr} \quad (17)$$
$$V_{qr} = r_r.i_{qr} + p\lambda_{qr} - \omega_r \lambda_{dr} \quad (18)$$

Where, subscripts d and q denotes for direct and quadrature axes respectively, s and r are used to indicate stator and rotor quantity. λ is the flux linkage, and ω_r is the angular velocity of the rotor. r_s and r_r are stator and rotor resistance, respectively. v and i notation are used for voltage and current, r_s , r_r are the resistance and L_{ls} , L_{lr} are the self-inductance of the stator and the rotor. Magnetizing inductance, which is responsible for voltage build up and stabilization of generated voltage for the different conditions of the induction generator is denoted by L_m . The generated electromagnetic torque (T_e) can be calculated as a function of d-q axis rotor and stator current as follows.

$$T_e = 1.5\left(\frac{P}{2}\right).L_m\left[i_{sq}.i_{rd} - i_{sd}.i_{rq}\right] \quad (19)$$

Relationship between electromagnetic torque turbine speed and shaft torque is given by,

$$T_{shaft} = J\left(\frac{2}{p}\right)\left(\frac{d\omega_r}{dt}\right) + T_e \quad (20)$$

Whereas, *P*: Number of poles in induction machine; *J*: Moment of Inertia of the rotor in ($Kg - m^2$) and T_{shaft} : Shaft/Drive torque in (N-m).

3. CONTROL TECHNIQUES FOR STAND-ALONE WIND ENERGY CONVERSION SYSTEM (SWECS)

The control technique for proposed SWECS is aimed to meet the demand of dc load under varying wind profile. It comprises the charge controller circuitry for battery and pitch control for WT to confirm operation within the safe limit. Charging of battery is achieved using tip speed ratio (TSR) MPPT technique in a controlled manner through dc-dc converter. The TSR control technique is straightforward and simple. It compares optimum TSR with actual one by measuring wind and turbine speed and send the error to controller. Combined control logic developed for charge and pitch control ensure effective operation of the system against all possible turbulences in wind flow.

3.1. Charging Control of Battery Bank

In this particular system, two modes of battery charging, constant current (CC) and constant voltage (CV) are proposed. Mode of battery charging is decided by state of charge (SoC) of the battery. A battery generally charges at constant rate up to a definite level of SoC (90%-98%). In CC mode of operation, battery charges at fast rate while SoC and terminal output voltage keep on increasing. Changeover from CC to CV mode occurs when SoC of the battery arrives at

reference which is set at 98%. In CC mode a lot of existing power from wind is transferred to load whereas in CV mode battery charges at much slower pace to avoid battery from overcharging.

3.2. Control Scheme of dc-dc Converter Working as Charge Controller for Battery Bank

Control logic is developed to generate gate pulse for dc-dc converter according to battery state of charge (SoC). The control scheme continuously monitors and suitably adjusts the duty ratio of the dc–dc converter (fig. 5). Flow chart for proposed control strategy is shown in Fig. 4. Whenever SoC of the battery is below the reference point (98%), it is required to transfer the power from source as much as possible to charge the battery and meet the load demand.

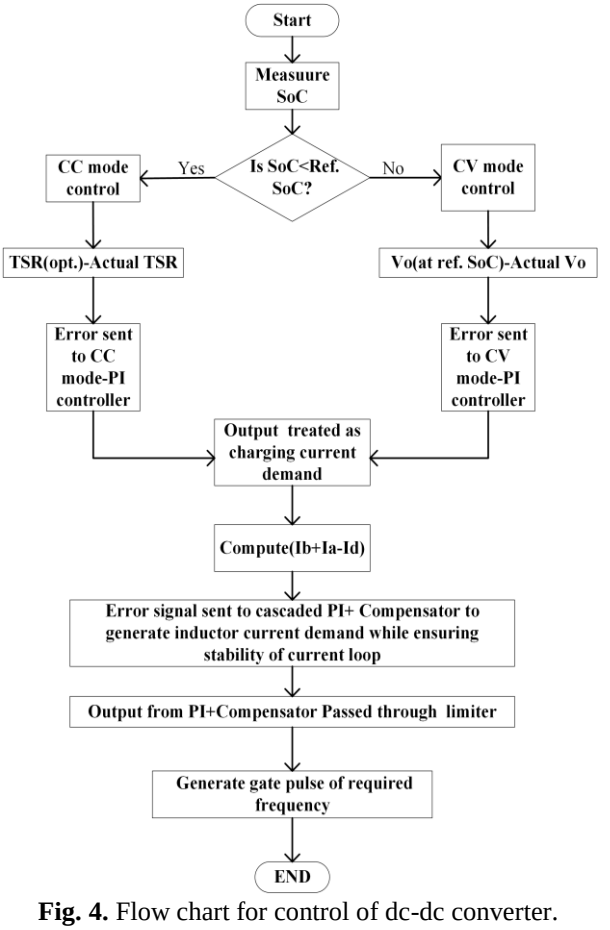

Fig. 4. Flow chart for control of dc-dc converter.

Wind turbine has to be operated at particular TSR value to capture the maximum possible power from wind. Value of optimum TSR (λ_{opt}) is obtained from the detailed method described in section 2.2. Actual value of TSR is compared with optimum one and error is sent to PI controller, which is tuned such as to generate demand for battery current. When SoC of the battery reaches above the reference value, CV mode control is activated which attempts to keep battery voltage at constant value consequently reducing charging current. In order to control the battery current, actual dc–dc converter output current (I_d)is compared with total output current (I_b+I_a) and error is sent to cascaded PI and phase compensator to generate required inductor current while ensuring stability of current control loop.

A. Design consideration for battery charging current control loop

To design the control scheme for battery current while ensuring the stability, it is important to present the model of the battery current control loop. Behavior of dc-dc converter output circuit shown in fig. 6 is analyzed in terms of 's' domain. Expressing in form of transfer taking all initial condition zero.

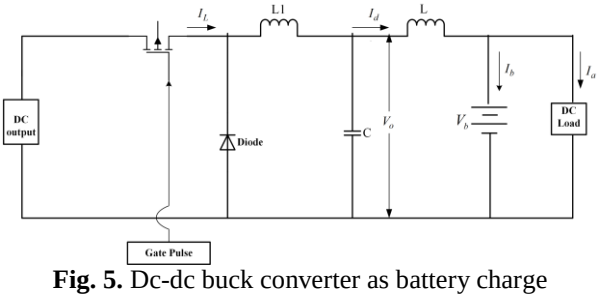

Fig. 5. Dc-dc buck converter as battery charge controller.

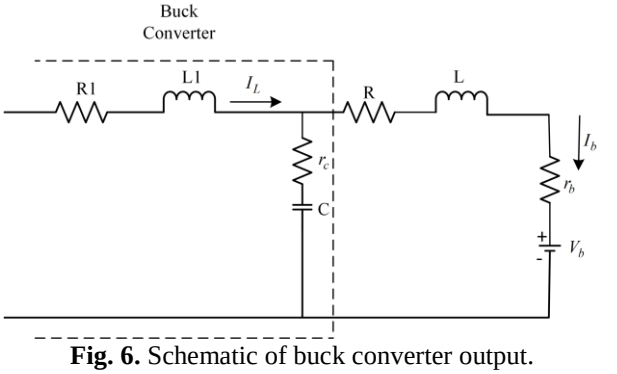

Fig. 6. Schematic of buck converter output.

Applying current divider rule in the circuit shown in fig. 6.

$$I_b(s) = I_L(s).\frac{r_c+{}^1/_{sC}}{sL+r_L+r_b+r_c+{}^1/_{sC}}$$

Or,

$$,\frac{I_b(s)}{I_L(s)} = \frac{r_c.sC+1}{LC.S^2+(r_L+r_b+r_c).sC+1} \quad (21)$$

r_L and r_c being small resistances are taken into account in series of the inductor and capacitor

respectively, whose value is taken as 1 mΩ each. Value of small series resistance of the battery denoted by r_b, is taken as 10 mΩ. After adopting the proper design procedure value of inductance and capacitance (L & C) are found to be 10.41mH and .75mF respectively considering chopping frequency as 2 kHz and peak to peak ripples are under the range of $\pm$2%. To design the proper controller for battery current, Bode diagram for battery-inductor current loop (equation (21)) is shown in fig.7. It may be observed that phase margin is 3.62^0 at 506 rad/s (80Hz). For a system to be stable, it should have positive gain margin and phase margin lying ideally in between 30^0-60^0.

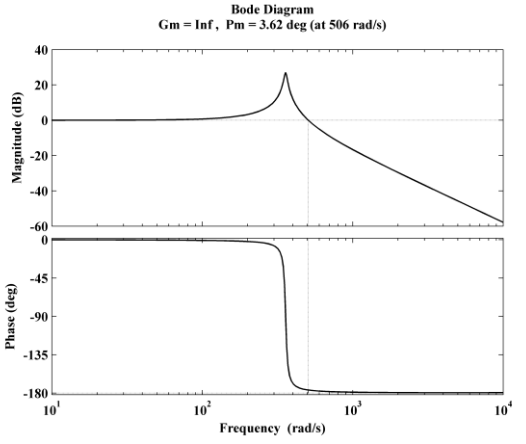

Fig. 7. Bode diagram of inductor- battery current loop.

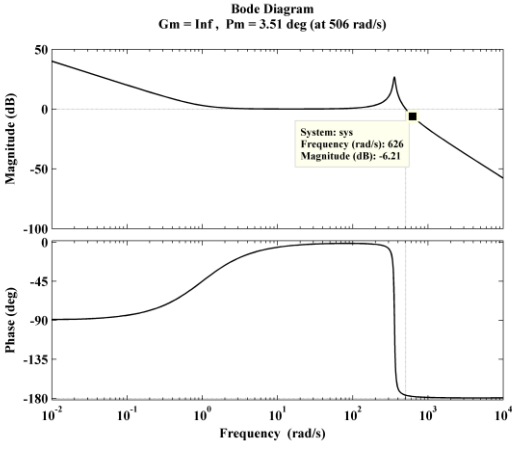

Fig. 8. Bode diagram of inductor- battery current loop with PI controller.

Therefore, there is need for phase lead contribution which could be achieved by using lead compensator. Moreover, the magnitude near the zero frequency region should be sufficient enough to achieve low steady error. In view of this a PI controller cascaded with lead compensator is designed properly to attain overall satisfactory performance for battery–inductor current control loop. Applying PI controller leads in increasing magnitude near zero frequency region from 0dB to 40 dB approximately (Fig. 8). Phase margin of current loop still need to be increased, hence lead compensator is used in conjunction with PI controller.

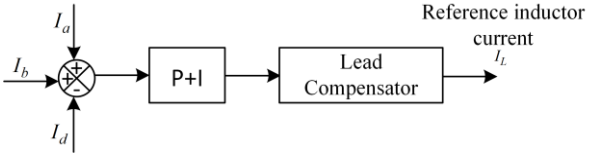

Fig. 9. Cascaded PI+ Lead compensator for battery-inductor current loop.

B. Design of Lead compensator (established on frequency response approach)

The main purpose of lead compensator is to remould the frequency response curve to provide required phase lead angle to compensate for phase lag accompanying with fixed system. Phase margin of 3.51 suggests that system is quite oscillatory. In order to keep phase margin between 30^0-60^0, lead compensator to be designed is expressed by transfer function as mentioned by equation (22).

$$G_c(s) = k_c.\alpha\frac{\tau s+1}{\tau s\alpha+1} = k_c.\frac{s+1/\tau}{s+1/\alpha\tau} = k_c.\frac{j\omega+1/\tau}{j\omega+1/\alpha\tau} \quad (22)$$

And phase angle,

$$\phi = \tan^{-1}\tau.\omega - \tan^{-1}\tau.\alpha.\omega \quad (23)$$

It is to be noted that maximum phase angle befalls at the geometric mean of the two corner frequencies, $1/\tau$ and $1/\alpha\tau$, i.e $\omega = 1/\tau.\sqrt{\alpha}$. Here, phase lead needed is assumed to be approximately 37^0. To attain the phase margin of 37^0, lead compensator has to provide the maximum desired phase angle, 37^0-3.51^0+4.5^0 $\cong$ 38^0 (4.5^0 has been introduced for the compensation of swing in gain crossover frequency). Maximum phase lead angle, $\emptyset_m$ can be expressed by the equation (24) as,

$$\sin\phi_m = \frac{1-\alpha}{1+\alpha} \quad (24)$$

α being attenuation factor can be found out as 0.24. The magnitude of lead compensator at maximum lead frequency is given by,

$$\left|\frac{1+j\omega\tau}{1+j\omega\alpha\tau}\right|_{\omega=1/\tau.\sqrt{\alpha}} = \frac{1}{\sqrt{\alpha}} = \frac{1}{0.49} = 6.2dB$$

Which corresponds to 626 rad/s (Fig. 8). This frequency is chosen as fresh gain cross over frequency (ω_c).Therefore, two corner frequency can be obtained as $\omega_c.\sqrt{\alpha}$ and $\omega_c/\sqrt{\alpha}$. Which can be calculated as 306.67 and 1277.8 respectively. Hence, transfer function of lead compensator can be given by:

$$G_c(s) = k_c.\frac{s+306.67}{s+1277.8} \tag{25}$$

Overall transfer function of inductor battery current loop with cascaded PI and compensator shown in fig. 9 can be represented by modifying equation (21).

$$\frac{I_b}{I_L} = K_c.\frac{s+1/\tau}{s+1/\alpha\tau}.\left(k_p+\frac{k_i}{s}\right).\frac{r_c.sc+1}{Lcs^2+(r_L+r_b+r_c).sc+1} \tag{26}$$

Equation (26) is simplified by taking the values from table 1. and written as,

$$\frac{I_b}{I_L} = \frac{1.5s^3+2\times10^6 s^2+6.14\times10^8 s+6.12\times10^8}{7.5s^4+9586s^3+1.011\times10^6 s^2+1.277\times10^9 s} \tag{27}$$

Bode diagram of modified inductor battery current control loop is depicted in Fig. 10. The design procedures yield the desired phase margin of 37.3 degree. All the design requirements of inductor battery control loop discussed previously are obtained.

Table 1. Charge controller parameter.

Parameter of charge controller	Value
K_c	2
K_p	1
K_i	1
L	10.41mH
C	0.75mF
r_L, r_c	1 mΩ
r_b	10 mΩ

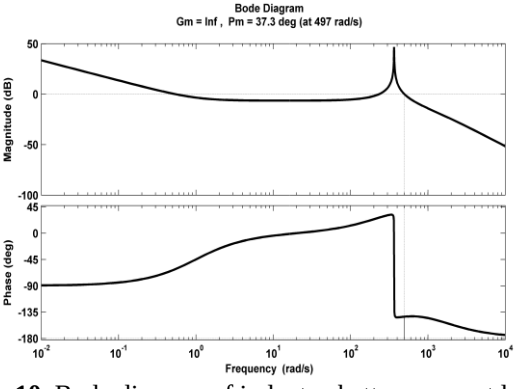

Fig. 10. Bode diagram of inductor-battery current loop with cascaded PI and lead compensator.

4. PITCH CONTROL

According to the wind speed, the variable-pitch WT systems generally have two operating regions, the partial-load region and full–load region.

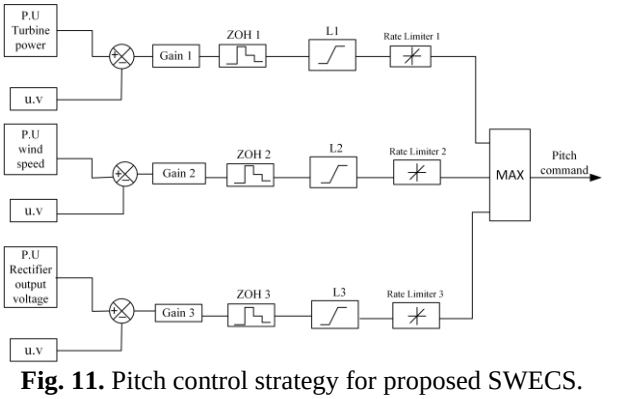

Fig. 11. Pitch control strategy for proposed SWECS.

In the partial load region actual wind speed is lower than rated wind speed. On the other side, in full load region where actual wind speed is higher than rated one, turbine ought to be protected from over angular speed. Nowadays, the cut-off speed of advanced wind turbine is greater than rated wind speed. If the wind turbine is made to operate over whole regions, then it may cause permanent damage to turbine shaft and blades. In addition to that, a standalone WECS have to supply fixed amount of limited power which may increase in case of excess of wind speed. In view of these facts, pitch control mechanism is important aspect in standalone WECS for restricting the wind power seized by the WT at the high-wind speed regions and providing safety to the system.

4.1. Pitch Control Strategy

The relationship between power-coefficient (C_p) versus (tip speed ratio (TSR) at different pitch angle is shown in Fig. 2. It can be observed that the value of C_p is maximum at zero degree. It decrases with the increase of the value of pitch angle. Lesser value of C_p indicates

less output turbine power due to reduced rotational speed of turbine. Thus in the case when angular speed of WT exceeds rated value pitch angle needs to increase accordingly. In proposed work, parameter of WT as well as electrical (rectifier output voltage) are taken into account for implementing pitch control scheme. Per unit value of each parameters including turbine power, wind speed, and rectifier output voltage are compared with their unit values and difference is passed through cascaded arrangement of several blocks as shown in fig. 11. Signals are passed through limiter whose lower limit is set at zero. Each of the values is passed to MAX block which selects the maximum output of the three to generate the pitch command. This arrangement provides protection from overvoltage and over-speeding of turbine blade by generating proper pitch command when any of the mentioned parameter goes beyond the rated limit.

5. RESULTS AND DISCUSSION

WECS is intended to meet the demand of standalone dc load under varying wind and load profile. It should be efficient enough to ensure uninterrupted power supply to the load. The aim is achieved by integrating battery with wind turbine system coupled with suitable power electronics circuit and control logic. Charge control (through tip-speed ratio) and pitch control logic are incorporated as control strategy in proposed wind energy conversion system. The system is tested under varying wind and load profile. Several WT turbine parameter like pitch angle, WT power, TSR and rotor and turbine shaft speed are investigated under various wind profile. In addition to this, variation of parameter such as battery SoC, current and voltage are also examined under changing wind speed. Two types of wind profiles are taken into consideration: (a) constant rise and fall (Fig. 12(a); (b) Mixed variation in wind speed in form of step and random change (Fig. 13(a). Efficacy of whole system is validated through simulation. Fig. 12(a) shows constant rise of wind speed 4m/s to 14m/s in 0-14 sec and fall from 16 m/s to 6 m/s in next 16-30 sec. Maximum value of wind speed (14m/s) stays constant for 2 seconds in the time interval of 14 to 16 seconds. In Fig. 13(a) two type of wind speed profile are considered for study of different parameters in simulation time of 30 minutes. In first 20 seconds wind speed profile undergo step variation while in next 10 seconds it is subjected to random variation having peak of 15m/s at 25th second. WECS is attached with load which is varied in step from 0 to 4kw.To observe the variation of different parameter under varying wind and load profile, the simulation is carried out for 30 seconds. It can be observed that whenever the velocity of wind exceeds 10m/s (rated value), pitch control mechanism is activated and as a result some pitch angle command is generated which control the power by reducing the turbine angular velocity. It can be noted from Fig. 12-13 that pitch angle remains at zero degree as far as wind speed is below the rated value (10m/s). It attains some positive value as speed exceeds 10m/s. All the variations in wind turbine parameter i.e TSR, shaft speed, p.u. generator speed, WT power can be seen with the variation in wind speed. To implements MPPT, value of TSR is tried to be maintained at its optimal value as derived in equation (14). Thus, maximum power is extracted by WT at all instant of time in order to meet the requirement of the load and charge the battery bank. Priority has been given to fulfil load demand than battery charging in case of insufficient wind power is available. When load demand is high and wind power is sufficiently enough, system transfer power to load as possible and charges battery at slower pace thereby increasing its SoC. In the case where wind power is not sufficiently available to meet the load demand, battery starts discharging so its SoC. Charging and discharging of the battery purely depends upon available wind power, load and battery SoC. There is also limitation on charging and discharging rate of the battery, controller ensures that maximum battery current should not go beyond ± 50 A (C/10). Efficacy of the whole system is verified through simulation in all possible wind speed condition (Fig. 12-13).

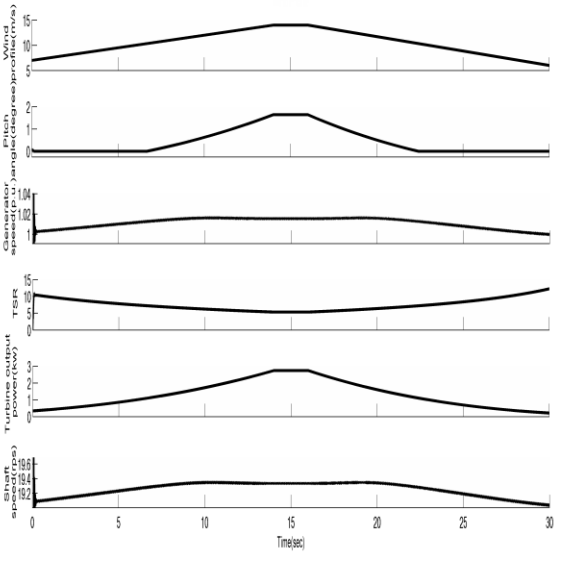

(a)

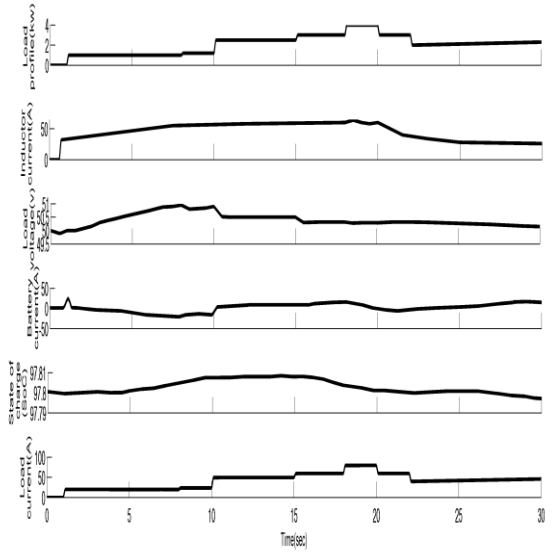

(b)

Fig. 12. (a) Variation of various parameter of WT system as well as (b) battery, converter and load under constant rise and fall of wind speed.

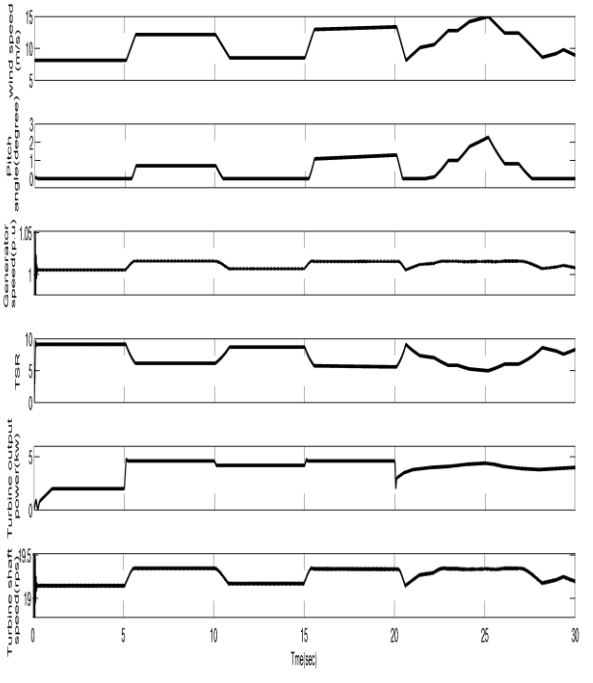

(a)

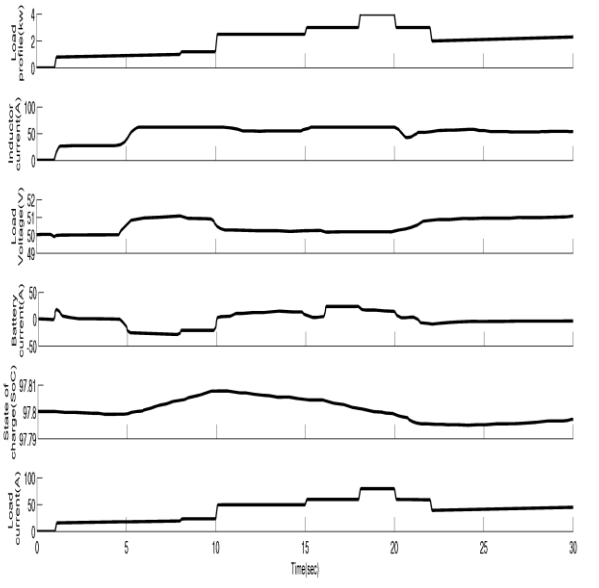

(b)

Fig. 13. (a) Variation of various parameter of WT system as well as (b) battery, converter and load under random wind speed.

6. CONCLUSION

The work proposes a standalone wind energy conversion system (SWECS) to extract the power from abundantly available wind energy. It consists of hybrid wind-battery system with suitable power electronics and control strategy to power varying dc load. In this work composite control strategy of battery charging and pitch angle control is demonstrated. Charging control is achieved with the inclusion of MPPT by comparing actual TSR with optimal one and sending signal to dc-dc converter after passing through properly designed PI controller and compensator. Pitch control is used for providing electrical and mechanical safety to WECS and balance power mismatch. In the eventuality, when power available from source after MPPT is higher than load demand, pitch angle control mechanism generates appropriate pitch angle command to lessen the rotational speed of WT. Efficacy of the whole system is confirmed through MATLAB simulation by creating different type of wind and load profile. Proposed system would be useful for harnessing wind energy and producing electricity for standalone application at remote place like sea shore hotels and small manufacturing unite where connection to grid is not possible due to any reason.

REFERENCES

[1] John K. Kaldellis, D. Zafirakis, **"The Wind Energy Evolution: A Short Review of a Long History",** *Renewable Energy*, Vol. 36, Issue 7, pp. 1887-1901, July 2011.

[2] Devashish, A. Thakur, S. Panigrahi and R. R. Behera, "**A Review On Wind Energy Conversion System and**

Enabling Technology," *International Conference on Electrical Power and Energy Systems (ICEPES)*, Bhopal, 2016, pp. 527-532.

[3] Devashish and A. Thakur, **"A Comprehensive Review on Wind Energy Systems for Electric Power Generation: Current Situation and Improved Technologies to Realize Future Development,"** *International Journal of Renewable Energy Research-IJRER*, Vol. 7, No. 4, pp. 1786-1805, December 2017.

[4] M. T. Ameli, S. Moslehpur, and A. Mirzale, **"Feasibility Study for Replacing Asynchronous Generators with Synchronous Generators In Wind Farm Power Stations,"** *in Proc. IAJC – IJME, Int. Conf. Eng. Technol., Music City Sheraton, Nashville*, TN, US, ENT pp. 17–19, 2008.

[5] A. Mesemanolis, C. Mademlis and I. Kioskeridis, **"High-Efficiency Control for a Wind Energy Conversion System with Induction Generator,"** *IEEE Transactions on Energy Conversion*, Vol. 27, No. 4, pp. 958-967, Dec. 2012.

[6] A. Mesemanolis, C. Mademlis and I. Kioskeridis, **"Optimal Efficiency Control Strategy in Wind Energy Conversion System with Induction Generator,"** *IEEE Journal of Emerging and Selected Topics in Power Electronics*, Vol. 1, No. 4, pp. 238-246, Dec. 2013.

[7] G. K. Singh, **"Self Excited Generator Research—A Survey,"** *Electric Power Syst. Res*., Vol. 69, No. 2/3, pp. 107–114, 2004.

[8] F. Blaabjerg, M. Liserre and K. Ma**, "Power Electronics Converters for Wind Turbine Systems,"** *IEEE Transactions on Industry Applications*, Vol. 48, No. 2, pp. 708-719, March-April 2012.

[9] A. M. D. Broe, S. Drouilhet, and V. Gevorgian, **"A Peak Power Tracker for Small Wind Turbines in Battery Charging Applications,"** *IEEE Tranaction on Energy Conversion*, Vol. 14, No. 4, pp. 1630–1635, Dec. 1999.

[10] Dipesh Kumar, Kalyan Chatterjee, **"A Review of Conventional and Advanced MPPT Algorithms for Wind Energy Systems,"** *Renewable and Sustainable Energy Reviews*, Vol. 55, pp. 957-970, 2016.

[11] Kot, R., M. Rolak, and M. Malinowski. **"Comparison of Maximum Peak Power Tracking Algorithms for a Small Wind Turbine."** *Mathematics and Computers in Simulation*, vol. 91, pp. 29-40, 2013.

[12] R. Datta and V. T. Ranganathan**, "A Method of Tracking the Peak Power Points for A Variable Speed Wind Energy Conversion System,"** *IEEE Transaction Energy Conversion*, Vol. 18, No. 1, pp. 163–168, Mar. 2003.

[13] S. M. R. Kazmi, H. Goto, G. Hai-Jiao, and O. Ichinokura, **"A Novel Algorithm for Fast and Efficient Speed-Sensorless Maximum Power Point Tracking in Wind Energy Conversion Systems,"** *IEEE Tranaction Industrial Electronics*, Vol. 58, No. 1, pp. 29–36, Jan. 2011.

[14] M. Chinchilla, S. Arnaltes, and J. C. Burgos, **"Control of Permanent Magnet Generators Applied to Variable-Speed Wind-Energy Systems Connected to the Grid,"** *IEEE Transaction Energy Conversion.*, Vol. 21, No. 1, pp. 130– 135, Mar. 2006

[15] P. Ching-Tsai and J. Yu-Ling, **"A Novel Sensorless MPPT Controller for a High-Efficiency Microscale Wind Power Generation System,"** *IEEE Transaction Energy Conversion*., Vol. 25, No. 1, pp. 207–216, Mar. 2010.

[16] V. Agarwal, R. K. Aggarwal, P. Patidar and C. Patki, **"A Novel Scheme for Rapid Tracking of Maximum Power Point in Wind Energy Generation Systems,"** IEEE Transactions on Energy Conversion, Vol. 25, No. 1, pp. 228-236, March 2010.

[17] M. Nasiri, J. Milimonfared, S.H. Fathi, **"Modeling, Analysis and Comparison of TSR and OTC Methods for MPPT and Power Smoothing in Permanent Magnet Synchronous Generator-based Wind Turbines,"** *Energy Conversion and Management*, Vol. 86, pp. 892-900, 2014.

[18] K. Y. Lo, Y. M. Chen, and Y. R. Chang, **"MPPT Battery Charger for Standalone Wind Power System,"** *IEEE Transaction Power Electronics*, Vol. 26, No. 6, pp. 1631–1638, Jun. 2011.

[19] Minh Quan Duong, Francesco Grimaccia, Sonia Leva, Marco Mussetta, Emanuele Ogliari, **"Pitch Angle Control Using Hybrid Controller for All Operating Regions of SCIG Wind Turbine System"**, *Renewable Energy*, Vol. 70, 2014, pp. 197-203.

[20] Civelek, Zafer, Murat Lüy, Ertuğrul Çam, and Necaattin Barışçı. **"Control of Pitch Angle of Wind Turbine by Fuzzy PID Controller."** *Intelligent Automation & Soft Computing*, Vol. 22, No. 3, pp. 463-471, 2016.

[21] A. S. Satpathy, N. K. Kishore, D. Kastha and N. C. Sahoo, **"Control Scheme for a Stand-Alone Wind Energy Conversion System,"** *IEEE Transactions on Energy Conversion*, Vol. 29, No. 2, pp. 418-425, June 2014.

[22] T. L. Van, T. H. Nguyen and D. C. Lee, **"Advanced Pitch Angle Control Based on Fuzzy Logic for Variable-Speed Wind Turbine Systems,"** *IEEE Transactions on Energy Conversion*, Vol. 30, No. 2, pp. 578-587, June 2015.

[23] Paul. C. Krause, Oleg Wasynczuk & Scott D. Sudhoff, **"Analysis of Electric Machinery",** *IEEE Press*, 1994.

[24] Muhammad H. Rashisd, **"Power Electronics Handbook,"** *Third edition, Academic press*, 2010.